Zika virus detection using antibody-immobilized disposable cover glass and AlGaN/GaN high electron mobility transistors

Jiancheng Yang, Patrick Carey, Fan Ren, Michael A. Mastro, Kimberly Beers, S. J. Pearton, and Ivan I. Kravchenko
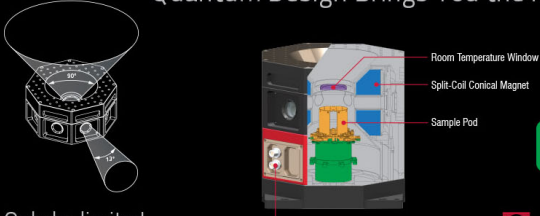
Zika virus detection using antibody-immobilized disposable cover glass and AlGaN/GaN high electron mobility transistors

Jiancheng Yang,[1] Patrick Carey IV,[1] Fan Ren,[1,a)] Michael A. Mastro,[2] Kimberly Beers,[3] S. J. Pearton,[3] and Ivan I. Kravchenko[4]

[1]Department of Chemical Engineering, University of Florida, Gainesville, Florida 32611, USA
[2]U.S. Naval Research Laboratory, Washington, DC 20375, USA
[3]Department of Materials Science and Engineering, University of Florida, Gainesville, Florida 32611, USA
[4]Center for Nanophase Materials Sciences, Oak Ridge National Laboratory, Oak Ridge, Tennessee 37830, USA

Zika virus detection was demonstrated using antibody-functionalized cover glasses externally connected to the gate electrode of an AlGaN/GaN high electron mobility transistor (HEMT). A pulsed bias voltage of 0.5 V was applied to an electrode on the region of the cover glass region functionalized with antibody, and the resulting changes of drain current of the HEMT were employed to determine the presence of Zika virus antigen concentration ranging from 0.1 to 100 ng/ml. The dynamic and static drain current changes as a function of Zika virus concentration were modeled with a spring-like elastic relaxation model and the Langmuir extension model, respectively. Excellent fits to the data were found with relaxation time constants of antibody and antigen molecules in the range of 11 μs and 0.66–24.4 μs, respectively, for the concentration range investigated. The ratio of antibody bound with antigen to the total available antibody on the functionalized contact window was in the range of 0.013–0.84 for the Zika antigen concentration range of 0.1–100 ng/ml. Since the HEMT is not exposed to the bio-solution, it can be used repeatedly. The functionalized glass is the only disposable part in the detection system, showing the potential of this approach for hand-held, low cost sensor packages for point-of-care applications. *Published by AIP Publishing.*
https://doi.org/10.1063/1.5029902

The Zika virus (ZIKV) is a flavivirus similar to West Nile virus, dengue, or yellow fever. The virus is primarily transmitted via the *Aedes* mosquito. Zika has been associated with improper brain development in fetuses—retinopathy, brain calcification, and microcephaly.[1–3] The ZIKV is a positive single stranded RNA with an open reading frame of 5′-C-prM-E-NS1-NS2A-NS2B-NS3-NS4A-NS4b-NS5-3′.[4,5] The NS1 protein was selected as the appropriate target for sensing, as it is excreted from infected cells in the form of a trimer and is found in the plasma membrane of infected cells.[6] The NS1 protein's function is related to flaviviral replication, immune evasion, and pathogenesis; however, the exact function is not understood and has only been extrapolated recently from comparison to the NS1 protein in West Nile and Dengue.[4–7] The structure of the ZIKV has been well documented with the recent advances in cryo-electron microscopy, which obtained a few Å level resolution. These advances allow for detailed analysis of protein folding, mapping, and initial investigations into the individual protein function.[8–11] Currently, no treatment is available for affected individuals with Zika other than bed rest, hydration, and nutrition.

Current studies showed that ZIKV can be detected by using[8–12] RNA in human urine, serum, and saliva specimens using the reverse transcription polymerase chain reaction (RT-PCR) method. However, the detection results were only robustly positive for urine testing using this highly sensitive RT-PCR method.[13] Another ZIKV detection method has

focused on testing of human saliva, with the peptidome analysis using mass spectrometry (MS/MS). Yet, when using PCR to identify a specific structural protein in the saliva for detection, there were no positive results from this testing due to the degradation of RNA in saliva during the saliva collection, storage, and processing.[14] Reverse transcription loop-mediated isothermal amplification (RT-LAMP) was also used to detect ZIKV RNA in unprocessed biological samples like urine, plasma, and Zika infected mosquito carcasses, with a detection limit of 0.71 pfu.[15] All of these methods are time consuming and require a well-trained technician to perform and complete the tests. Thus, there is a strong need to develop a rapid and reliable ZIKV detection technique. A reliable bio-sensor that would provide rapid, accurate blood ZIKV concentration without any centrifuge and dilution would be a ground-breaking technology for determining whether a patient is infected with the ZIKV.

There has been strong interest in electronic detection approaches for viruses, using biologically functionalized field effect transistors (bio-FETs). The graphene-based field effect biosensor has been demonstrated recently for Zika Virus detection with an antibody and antigen interaction mechanism.[16] One attractive approach is the use of AlGaN/GaN high electron mobility transistors (HEMTs) functionalized with antibody or aptamer over the active gate channel.[17–22] The AlGaN/GaN HEMTs have demonstrated superior bio-sensing characteristics due to a high density two-dimensional electron gas (2DEG) channel located close the surface (around 25 nm) and very sensitive to changes in surface charges.[21–27] However, for conventional AlGaN/GaN HEMT

a)fren@che.ufl.edu

bio-sensing applications with the antibody immobilized directly over the active gate channel, the detection would not be very consistent for high ionic strength solutions such as human blood or serum. This is due to the high charge screening effect in high ionic strength solutions, where the Debye length is much shorter than the antibody.[22,24] To overcome this challenge, Hsu *et al.*[22] and Sarangadharan *et al.*[24] reported double pulse measurements using AlGaN/GaN HEMT biosensors, with an electrical double layer approach in which the functionalized gate electrode is spatially separated from the active gate channel area to eliminate these charge screening effects in high ionic strength solutions. This allows the measurements to be performed without any dilution or washing process.[22,24]

In this work, a disposable cover glass externally integrated with an AlGaN/GaN HEMT was employed to detect the ZIKV. Two metal electrodes were fabricated on the glass: one of them functionalized with antibody and the other one connected to the gate side of the HEMT device. The functionalized electrode was exposed to different concentrations of ZIKV solution. During application of a pulsed voltage to the electrode functionalized with antibody, the time dependent drain currents of HEMT were monitored, and the changes in drain current were used to determine the ZIKV concentrations. A spring-like elastic relaxation model and the Langmuir extension model were used to simulate the dynamic and static drain current responses, respectively, with excellent fits to the experimental data. The dynamic and static drain currents were defined as the time dependent drain current and the drain current at chosen specific time.

Figure 1 shows the schematic of the sensor set-up, which consists of an antibody functionalized cover glass and an AlGaN/GaN HEMT. The AlGaN/GaN HEMT structure is grown on a sapphire substrate with a low temperature AlN nucleation layer, 2.2 μm undoped GaN buffer layer, and 25 nm $Al_{0.25}Ga_{0.75}N$ barrier layer by metal organic chemical vapor deposition. Device isolation was achieved with a Cl_2/Ar discharge in a Plasma Therm 790 inductively coupled

plasma (ICP) system with 200 W ICP power and 50 W rf power at 2 and 13.56 MHz, respectively. The source and drain Ohmic contacts were formed by e-beam evaporation with Ti/Al/Ni/Au (25/125/45/100 nm) with a standard lift-off process, and the contacts were annealed at 850 °C for 45 s. Schottky gate contacts were formed with e-beam deposition Ni/Au (20 nm/80 nm). Ti/Au was used as interconnection metals.

For the cover glass portion, two 100 μm wide metal lines of Ni/Au (20 nm/80 nm) separated by 20 μm were fabricated using e-beam evaporation and standard lift-off. A 100 nm SiN_x passivation layer was deposited with a plasma enhanced chemical vapor deposition system to passivate the metal electrodes, and a 100 μm $\times$ 100 μm contact window was opened on both metal electrodes with buffered oxide etch (BOE). One of the contact windows was treated with 1 mM of thioglycolic acid (TGA) for 12 h by covering the other contact window with the photoresist. The TGA thiol group strongly interacts with and bonds to the Au surface, which was previously verified by X-ray photoelectron spectroscopy.[27] The excess TGA molecules were rinsed off with de-ionized water, and the photoresist was stripped with acetone. 100 μg/ml Zika antibody solution (recombinant Zika NS1) was introduced to the contact window coated with TGA, and the samples were stored at 4 °C for 2 h. The carboxyl functional group of the TGA molecules reacted to the amines on the Zika antibody. The antibody reacting with the carboxyl functional group was previously studied by atomic force microscopy, which showed the average height of the antibodies of around 4.2 nm.[28] Then, the cover glass was rinsed with deionized (DI) water and 10 nM phosphate-buffered saline (PBS) solution to remove any unbonded Zika antibody molecules.

To test the Zika antigen concentration, the time dependent HEMT drain current was measured at room temperature using a Keysight B1500 parameter analyzer. A Keysight B1530 pulse generator was employed to provide a 60 μs pulsed voltage of 2 V on the drain of the HEMT and a synchronized 50 μs pulsed voltage of 0.5 V on the Zika antibody immobilized electrode with 5 μs delay after biasing the drain electrode with a Keysight B1530 pulse generator, as shown in Fig. 1. The target Zika antigen (Recombinant Zika Virus NS1) solutions with an isoelectric point of 5.8 were diluted with 2 wt. % Tween 20 and 0.5 wt. % bovine serum albumin (BSA) in pF 7.4 PBS solution with 0.1, 1, 10, or 100 ng/ml concentration. We employed 5 min of buffering time for the Zika antigen to bind to the recombinant Zika NS1 protein before each target concentration measurement. Five devices of each type were tested, and each data point represents the average of five measurements from each of these devices.

Figure 2(a) shows the time dependent HEMT drain current responses to 0.5 V of 50 μs pulsed voltage applied to the electrode functionalized with Zika antibody. There were two distinct characteristics observed for the dynamic drain current response after applying +0.5 V pulsed voltage. First, the static drain current increase during the entire period of 50 μs was dependent on the Zika antigen concentration applied on the contact window of the glass sample; for higher Zika antigen concentrations, larger increases of drain current were observed. For the time dependent drain current, within this
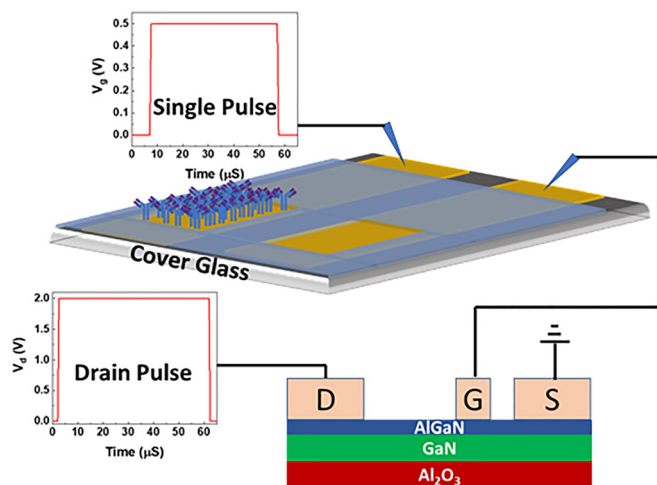

FIG. 1. Schematic of a Zika virus sensor with a cover glass functionalized with Zika antibody in a 100×100 μm^2 area and separated by 20 μm from a bare electrode externally connected with a HEMT. A 0.5 pulsed gate voltage (V_G, 50 μs duration) was applied to the electrode fabricated on the cover glass and functionalized with Zika antibody, while a pulsed drain voltage (V_D, 60 μs duration) of 2 V was applied to the drain of HEMT.
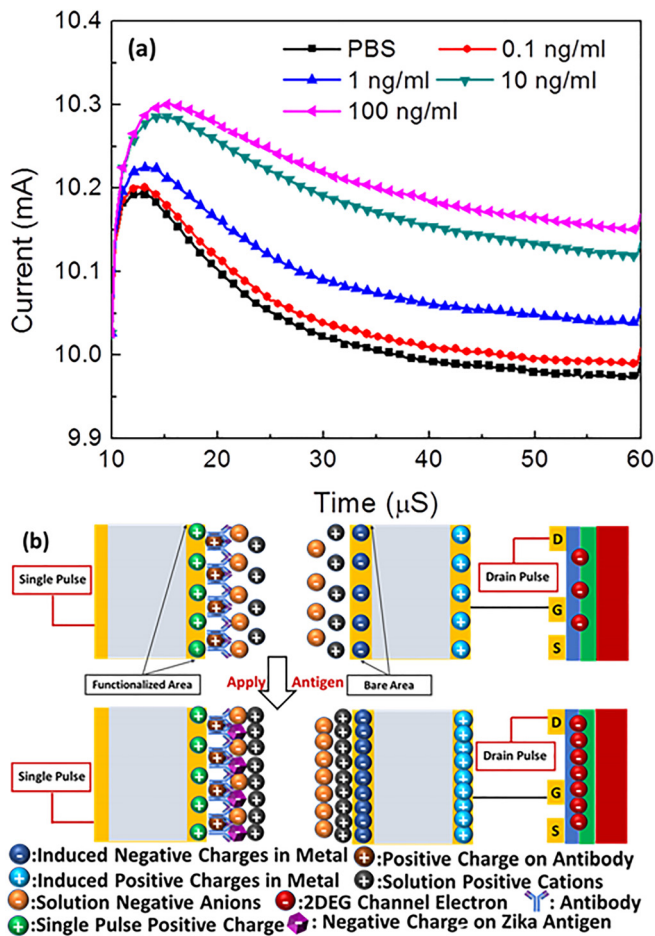
FIG. 2. (a) Time dependent drain currents for the cover glass exposed to blank 1X PBS, Tween 20, and 1% BSA and such PBS with different antigen concentrations. (b) Schematic of distribution of induced charges on the metal electrode, charges in the solution around the vicinity of the electrode, and negative charges on the antibody and antigen molecules. The HEMT structure consists of AlGaN/GaN layers on a sapphire substrate and source (S), drain (D), and gate (G) contacts.

$50\,\mu$s period, the drain current suddenly increased within $5\,\mu$s after applying 0.5 V pulsed voltage and then gradually leveled off.

The higher drain current corresponding to the $50\,\mu$s pulsed voltage applied to the electrode functionalized with Zika antibody means that more positive charges are induced on the gate of HEMT due to charge neutralization on the electrodes on the glass, as well as in the PBS or PBS with different concentrations of the antigen solution electrode and the negative charges carried on the antibody and antigen. Since the isoelectric point of the antigen is 5.8 to compare with the isoelectric point of 7.4 for the reference PBS, the antigen would carry negative charges in the PBS with different concentrations of antigen solution applied on the contact windows of the glass. As shown in Fig. 2(b), the opposite-polarity electrical double-layers are induced on both functionalized and unfunctionalized windows as a result of the positive 0.5 V of single pulse and native charges on the antigen.[29] Due to charge neutralization in the PBS or PBS solution with different antigen concentrations, more positive charges in the solution accumulate on the metal electrode contact window without functionalized antibody, and negative charges are induced on the metal electrode next to the

solution with more positive charges. Since this metal electrode is externally connected to the gate of HEMT, more positive charges are induced by the negative charges on the metal electrode next to the solution via charge neutralization on the metal. For the PBS solutions applied on the glass sample with higher antigen concentrations, more antigen molecules with negative charge will bind to the antibody molecules. Thus, the drain current increase was proportional to the antigen concentration through charge neutralization in both solution and metal, with more positive charge inducing more positive charge on the gate of HEMT and producing higher drain currents.

The antigen and antibody binding occurs through active sites on these two protein molecules. This binding process was reversible, and the drain current change of HEMT induced by the different concentrations of antigen solution could be fit with the Langmuir Extension model shown in the following equation:

$$\Delta I = \frac{101 * [C]^{0.87}}{1 + 0.54 * [C]^{0.87}}, \tag{1}$$

where ΔI is the change in drain current between the target antigen solutions and baseline PBS solution at $50\,\mu$S in Fig. 2(a). [C] is the antigen concentration in ng/ml. As shown in Fig. 3, the modeled drain current change with different concentrations fits well with the experimental data, with error bars less than 5%.

For the time-dependent drain current, within this $50\,\mu$s period, the drain current abruptly increased after applying the 0.5 V pulsed voltage and then gradually leveled off. Since the antigen and antibody molecules carry negative charges, they will be attracted to the electrode functionalized with antibody by the $+0.5$ V pulsed voltage applied. Once these molecules reach the electrode, a repelling force builds as a result of the negative charges. These molecules would gradually relax, as shown in Fig. 3. The static drain current increases were induced by the negative charges on the
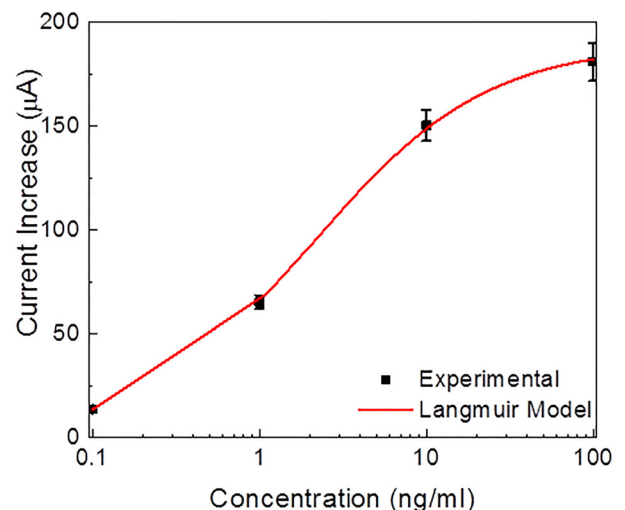

FIG. 3. Drain current increase (data point) for the cover glass exposed to different antigen concentrations (semi-log scale) as compared to the drain current for the cover glass exposed to the blank PBS solution and the simulated drain current increases with the Langmuir extension model.

antibody and antigen molecules. The drain current increases when both antibody and antigen molecules are attracted closer to the metal electrode upon the 0.5 V pulsed voltage and then progressively level off as an equilibrium is reached.

The protein structure has a variety of physical interactions with an applied electric-field in terms of stretching, shearing, bending, and contraction with breaking and re-forming of hydrogen bonds, local pH changes, and protein side-chain motions.[30] Such transformations of the protein configuration stimulated by the electric-field were modeled with a molecular dynamics simulation technique.[31] The Hookean spring model[32] was employed to simulate the relaxation portion of the time-dependent drain current. The dynamic equation of the mass-spring-damper model is given by

$$m\frac{d^2x(t)}{dt^2} + \varphi * \frac{dx(t)}{dt} + k * x(t) = 0, \qquad (2)$$

where m and k are the protein material properties, φ is the dragging coefficient associated with protein relaxation, t is the time, and x(t) is the stretched distance of the antibody and antigen under a certain electrical field and is proportional to the charges induced on the gate of HEMT. Since the drain current is proportional to the gate voltage of the HEMT or the stretched distance of the antibody and antigen molecules, the solution of Eq. (2) for the stretched distance is directly proportional to the drain current as

$$I_D(t) = (1 - c^*) * A * \exp\left(-\frac{t[\mu s]}{\tau_1}\right)$$
$$+ c^* * B * \exp\left(-\frac{t[\mu s]}{\tau_2}\right) + E, \qquad (3)$$

where c* is the ratio of antibody bound with antigen to the total available antibody on the functionalized contact window, τ_1 and τ_2 are the relaxation time constants of antibody and antigen molecules, respectively, and A, B, and E are the constants. c* mainly depends on the antigen concentration, and it can be related to ΔI through the Langmuir model. The fitting equation for c* and [C] is as follows:

$$c^* = \frac{0.14 * [C]^{1.33}}{1 + 0.17 * [C]^{1.33}}. \qquad (4)$$

Figure 4 shows the modeled drain current for PBS solution without antigen and PBS solutions with different antigen concentrations, and Table I lists the simulated time constants and ratio of antibody bound with antigen to the total available antibody. As shown in Fig. 4, the simulated time dependent drain current had an excellent fit with the experimental data. There was a 40× difference in the antigen relaxation time constant, τ_2, for the lower (0.66 μs at 0.1 ng/ml) and higher antigen concentrations (24.4 μs at 100 ng/ml), which could be due to additional interactions among antigen molecules for the higher antigen concentrations. Note that the ratio of antibody bound with antigen to the total available antibody on the functionalized contact window increased from 0.013 at 0.1 ng ml to 0.84 at 100 ng/ml, with the ratio scaling faster than the concentration due to increased interaction probability.
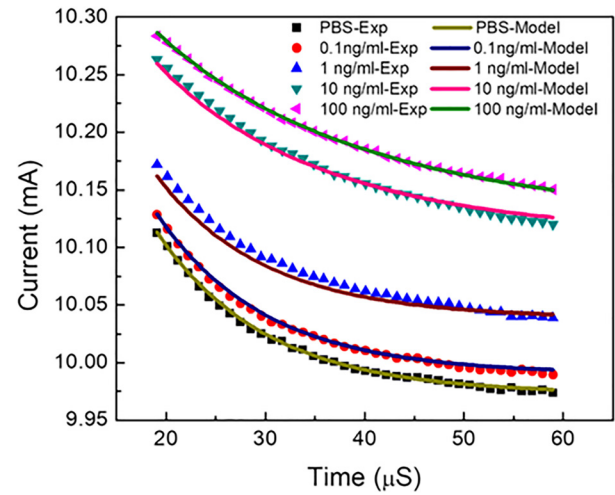

FIG. 4. Dynamic drain current (data point) for the cover glass exposed to different antigen concentrations and the simulated drain current with the spring relaxation model.

TABLE I. Ratio of antibody bound with antigen to the total available antibody on the functionalized contact window, c*, and relaxation time constants of antibody and antigen molecules, τ_1 and τ_2, respectively, as a function of Zika antigen concentration.

Zika concentration [C] (ng/ml)	c*	τ_1 (μs)	τ_2 (μs)
0 (PBS, BSA, Tween 20)	0.00	10.97	…
0.1	0.013	…	0.66
1	0.12	…	1.01
10	0.67	…	22.22
100	0.84	…	24.39

In summary, a rapid, low cost, bio-sensor for ZIKV was demonstrated by integrating a disposable cover glass with metal electrodes with an AlGaN/GaN HEMT. The HEMT is not exposed to any chemicals and can be reused. A wide range of Zika antigens, 0.1–100 ng/ml, were detected. The Langmuir extension model and spring-like elastic relaxation models provided excellent fits to the experimental static and dynamic drain currents upon pulsed biasing of the electrode fabricated on the cover glass and functionalized with Zika antibody.

[1]J.-D. Fine and K. A. Arndt, J. Am. Acad. Dermatol. **12**, 697 (1985).
[2]M. Onorati, Z. Li, F. Liu, A. Sousa, N. Nakagawa, M. Li, M. Dell'Anno, F. Gulden, S. Pochareddy, A. Tebbenkamp, W. Han, M. Pletikos, T. Gao, Y. Zhu, C. Bichsel, L. Varela, K. Szigeti-Buck, S. Lisgo, Y. Zhang, A. Testen, X. Gao, J. Mlakar, M. Popovic, M. Flamand, S. Strittmatter, L. Kaczmarek, E. Anton, T. Horvath, B. Lindenbach, and N. Sestan, Cell Rep. **16**, 2576 (2016).

[3]F. Lum, D. Low, Y. Fan, J. Tan, B. Lee, J. Chan, L. Rénia, F. Ginhoux, and L. Ng, Clin. Infect. Dis. **64**, 914 (2017).

[4]T. Chambers, Annu. Rev. Microbiol. **44**, 649 (1990).

[5]Y. Shi and G. Gao, Trends Biochem. Sci. **42**, 443 (2017).

[6]H. Song, J. Qi, J. Haywood, Y. Shi, and G. Gao, Nat. Struct. Mol. Biol. **23**, 456 (2016).

[7]R. Hilgenfeld, EMBO J. **35**, 2631 (2016).

[8]S. Badshah, A. Naeem, and Y. Mabkhot, Viruses **9**, 7 (2017).

[9]V. Prasad, A. Miller, T. Klose, G. Sirohi, G. Buda, W. Jiang, R. Kuhn, and M. Rossmann, Nat. Struct. Mol. Biol. **24**, 184 (2017).

[10]D. Sirohi, Z. Chen, L. Sun, T. Klose, T. Pierson, M. Rossmann, and R. Kuhn, Science **352**, 467 (2016).

[11]W. Saw, A. Pan, M. S. Manimekalai, and G. Grüber, Antiviral Res. **141**, 73 (2017).

[12]J. A. Priye, S. Bird, Y. Light, C. Ball, P. Negrete, and R. J. Meagher, Sci. Rep. **7**, 44778 (2017).

[13]A. M. Bingham, M. Cone, V. M. L. Heberlein-Larson, D. Stanek, C. Blackmore, and A. Likos, Morb. Mortal. Wkly. Rep. **65**, 475, 2016.

[14]D. Zuanazzi, E. J. Arts, P. K. Jorge, Y. Mulyar, R. Gibson, Y. Xiao, M. B. dos Santos, M. A. A. M. Machado, and W. L. Siqueira, J. Dent. Res. **96**, 1078 (2017).

[15]O. Yaren, B. W. Alto, P. V. Gangodkar, S. R. Ranade, K. N. Patil, K. M. Bradley, Z. Yang, N. Phadke, and S. A. Benner, BMC Infect. Dis. **17**, 293 (2017).

[16]S. Afsahi, M. B. Lerner, J. M. Goldstein, J. Lee, X. Tang, D. A. Bagarozzi, Jr., D. Pan, L. Locascio, A. Walker, F. Barron, and B. R. Goldsmith, Biosens. Bioelectron. **100**, 85–88 (2018).

[17]J. K. Y. Law, A. Susloparova, X. T. Vu, X. Zhou, F. Hempel, B. Qu, M. Hoth, and S. Ingebradt, Biosens. Bioelectron. **67**, 170 (2015).

[18]D. Sarkar, W. Liu, X. Xie, C. Aaron, A. C. Anselmo, S. Mitragotri, and K. Banerjee, ACS Nano **8**, 3992 (2014).

[19]S. Wustoni, S. Hideshima, S. Kuroiwa, T. Nakanishi, M. Hashimoto, Y. Mori, and T. Osaka, Biosens. Bioelectron. **67**, 256 (2015).

[20]H. H. Lee, M. Bae, S.-H. Jo, J.-K. Shin, D. H. Son, C.-H. Won, and J.-H. Lee, Sens. Actuators, B **234**, 316 (2016).

[21]B. S. Kang, H. T. Wang, F. Ren, and S. J. Pearton, J. Appl. Phys. **104**, 031101 (2008).

[22]C.-P. Hsu, P.-C. Chen, A. K. Pulikkathodi, Y.-H. Hsiao, C.-C. Chen, and Y.-L. Wang, ECS J. Solid State Sci. Technol. **6**, Q63 (2017).

[23]Y.-W. Kang, G.-Y. Lee, J.-I. Chyi, C.-P. Hsu, Y.-R. Hsu, C.-H. Hsu, Y.-F. Huang, Y.-C. Sun, C.-C. Chen, S. C. Hung, F. Ren, J. A. Yeh, and Y.-L. Wang, Appl. Phys. Lett. **102**, 173704 (2013).

[24]I. Sarangadharan, A. Regmi, Y.-W. Chen, C.-P. Hsu, P.-c. Chen, W.-H. Chang, G.-Y. Lee, J.-I. Chyi, S.-C. Shiesh, G.-B. Lee, and Y.-L. Wang, Biosens. Bioelectron. **100**, 282 (2018).

[25]J. C. Yang, P. Carey, F. Ren, Y. L. Wang, M. L. Good, S. Jang, M. A. Mastro, and S. J. Pearton, Appl. Phys. Lett. **111**, 202104 (2017).

[26]F. Ren and S. J. Pearton, Phys. Status Solidi C **9**, 393 (2012).

[27]B. S. Kang, S. J. Pearton, J. J. Chen, F. Ren, J. W. Johnson, R. J. Therrien, P. Rajagopal, J. C. Roberts, E. L. Piner, and K. J. Linthicum, Appl. Phys. Lett. **89**, 122102 (2006).

[28]V. Ierardi, F. Ferrera, E. Millo, G. Damonte, G. Filaci, and U. Valbusa, J. Phys.: Conf. Ser. **439**, 012001 (2013).

[29]C.-H. Chu, I. Sarangadharan, A. Regmi, Y.-W. Chen, C.-P. Hsu, W.-H. Chang, G.-Y. Lee, J.-I. Chyi, C.-C. Chen, S.-C. Shiesh, G.-B. Lee, and Y.-L. Wang, Sci. Rep. **7**, 5256 (2017).

[30]D. R. Hekstra, K. I. White, M. A. Socolich, R. W. Henning, V. Srajer, and R. Ranganathan, Nature **540**, 400 (2016).

[31]M. Hamdi, G. Sharma, A. Ferreira, and C. Mavroidis, in *Proceedings of the 2006 IEEE International Conference on Robotics and Automation* (ICRA) (2006), p. 1794.

[32]O. Chaudhuri, L. Gu, M. Darnell, D. Klumpers, S. A. Bencherif, J. C. Weaver, N. Huebsch, and D. J. Mooney, Nat. Commun. **6**, 6365 (2015).